

# Small-Signal Stability Verification Issues for Transmission Systems with Distributed Renewables

Richard Y. Zhang, Jorge Elizondo, James L. Kirtley Jr., Jacob K. White  
Department of Electrical Engineering & Computer Science  
Massachusetts Institute of Technology, Cambridge, MA 02139, USA  
{ryz, jelizon, kirtley, white}@mit.edu

**Abstract**—High penetrations of distributed renewables can dramatically increase uncertainty in the transmission system, making small-signal stability verification far more challenging. In this paper, we examine the impact of generating 30% of the power in the IEEE 118 bus test network with 118 distributed renewable sources, and show the inadequacy of sampling approaches to stability analysis. We show that multipoint local optimization can find less stable scenarios that are easily missed by sampling. In addition, we show that stability verification (or certification) is computationally tractable, but as yet, only by linearizing and dimension-reducing the parametric variation.

## I. INTRODUCTION

High penetrations of renewable energy resources will introduce unprecedented uncertainty to the power system, making stability analysis considerably more challenging. Previous studies have generally concurred that—assuming that sufficient inertia remains on the system—high penetrations of renewables generation would not significantly worsen small-signal stability in the *average-case scenario* [1], [2]. Considerably less is known in the *worst-case scenario*, whether it is possible for renewables to significantly impact stability, and how might such issues manifest.

One popular approach is to apply statistical, or “Monte Carlo” techniques, to the study of small-signal stability in the presence of uncertainty [3], [4]. By sampling the stability of selected or random scenarios, and by assuming a particular underlying distribution, a prediction interval can establish that stability is *expected* for, say, 99% of all possible scenarios. However, such predictions can often mislead if the impact of significant outliers are not adequately considered.

In this paper, we present a case study based on the IEEE 118-bus test system, in which 30% of the power is generated by distributed renewable generation added to each of the 118 buses, in order to highlight the challenge presented by outliers, and the importance of a certification approach. Statistical analysis shows the system to be stable and unassuming on average, with the boundary to instability located more than 6 standard deviations away. But using local optimization, we were able to find 100 unstable or nearly unstable scenarios, suggesting that outlier scenarios may be far more common than first appeared. Finally, a stability certificate for a low-dimensional, linearized version of our system model is computed, bounding the worst-case instability by a figure that is not too much worse than the unstable scenarios found via local optimization.

## II. THEORETICAL & COMPUTATIONAL TOOLS

### A. Eigenvalue Analysis

The time-domain dynamics of power systems are modeled using differential algebraic equations,

$$\dot{x} = f(x, y), \quad 0 = g(x, y), \quad (1)$$

in which  $x, y$  are state and algebraic variables, and  $f, g$  are nonlinear but smooth, differentiable functions. The point  $(x_0, y_0)$  is an equilibrium point if

$$f(x_0, y_0) = 0, \quad g(x_0, y_0) = 0,$$

and physically corresponds to a *power flow* solution over the network, i.e. the balancing of generated, consumed and transmitted complex power at every bus.

Small-signal stability at  $(x_0, y_0)$  can be analyzed by examining the *linear* differential-algebraic system,

$$\dot{\xi} = A\xi + B\eta, \quad 0 = C\xi + D\eta, \quad (2)$$

where  $\xi = x - x_0$  and  $\eta = y - y_0$ , and the matrices  $A, B, C, D$  are the Jacobians of the functions  $f$  and  $g$ , evaluated at  $(x_0, y_0)$ . The matrix  $D$  is nonsingular except in cases of voltage collapse, so stability can be equivalently assessed by examining the state-space model

$$\dot{\xi} = (A - BD^{-1}C)\xi. \quad (3)$$

It is common to quantify stability with a *decay rate*, in units of “fraction reduction per second”, by considering the lightest-damped eigenmode. Specifically, for  $\dot{x} = Mx$ , the damping rate,  $\alpha$ , is defined as

$$\alpha(M) = -\max_i \operatorname{Re} \lambda_i \{M\}. \quad (4)$$

A state-space model will asymptotically decay as  $\exp(-t\alpha(M))$  assuming  $\alpha(M) > 0$ , and is unstable if  $\alpha(M) \geq 0$ <sup>1</sup>.

<sup>1</sup>The damping ratio is a commonly-used alternative for quantifying stability, but can be treated similarly.

## B. Parametric Uncertainty & Statistical Analysis

A consequence of the uncertainty introduced by renewables is that the functions  $f, g$  in (1) are themselves uncertain. In turn, this implies that the equilibria of  $f, g$  are uncertain, as are their Jacobians  $A, B, C, D$  as evaluated about each equilibrium.

The uncertainty can be made deterministic through parameterization. For example, our latter case study introduces an uncertain parameter  $u_i$  for each renewable source considered, and uses it to scale the power output at that source. While the values of the parameters  $u \in \mathbb{R}^m$  are themselves uncertain, the relationship between the parameters and the corresponding model functions  $f_u$  and  $g_u$  is deterministic, as is the solution to the power flow equations and the Jacobians evaluated at the equilibrium, written  $A_u, B_u, C_u, D_u$ .

Our objective is to analyze the decay rate over all possible choices of the uncertain parameter  $u$ . Mathematically, the set of all possible decay rates  $\mathcal{D} \subset \mathbb{R}$  is defined

$$\mathcal{D} = \{\alpha(A_u - B_u D_u^{-1} C_u) : 0 \leq u_i \leq 1 \quad \forall i \in \{1, \dots, m\}\}.$$

While analyzing  $\mathcal{D}$  explicitly is very difficult, collecting samples from it is relatively straightforward, e.g. by selecting  $u$  from a uniform distribution. With enough samples, quantitative statements about stability can be made using statistical analysis. For example, the stability of the “average uncertain scenario” can be determined. Prediction intervals can also be computed by assuming an underlying distribution.

## C. Local Optimization

Statistical approaches can never be conclusive about *worst-case* behavior, but in this case study, the statistic approach is surprisingly misleading. Using the same notation as before, our objective is to compute the least-stable element of  $\min \mathcal{D}$ , equivalent to the constrained optimization problem

$$\begin{aligned} & \text{minimize} && \alpha(M_u) \\ & \text{subject to} && A_u - B_u D_u^{-1} C_u = M_u \\ & && 0 \leq u_i \leq 1 \quad \forall i \in \{1, \dots, m\}. \end{aligned} \quad (5)$$

The problem is nonlinear, nonconvex, nonsmooth and indeed, very ill-behaved. But finding locally optimal solutions is easy: a strictly feasible initial point can be incrementally improved, e.g. using a trust-region quasi-Newton’s method, until no further progress can be made. This suboptimal, local approach is ubiquitous in controller synthesis [5].

In the context of stability analysis, any insufficiently stable scenario found through local optimization immediately tells us that not all uncertain scenarios are acceptable; the worst-case is at least as bad the one found through optimization. However, the opposite is not necessarily true. Just because local optimization is unable to find an unstable scenario does not mean that one does not exist. We can only increase our chances of catching the worst-case by restarting the search at different initial points.

## III. CASE STUDY DESCRIPTION

In this paper, we study the IEEE 118 bus system in the context of achieving ~30% distributed renewable penetration, and the potential small-signal stability issues that may arise. First, three conventional generators (located at buses 10, 25 and 89) are retired from the system. Then, the displaced generation capacity (around 1,277 MW) is compensated by installing renewable generation at each of 118 buses throughout the system. In the “base case” scenario, the amount of distributed generation allocated to each bus is proportional to the size of the existing load, in order to reflect the fact that larger load centers tend to accrue more renewables.

The objective of our study is to simulate the uncertainty associated renewables generation, and to quantify its impact on system-wide small-signal stability. To this end, we parameterize the uncertainty of the renewable generation at each bus with its own uncertain variable,  $u_i$ , which ranges from 0 to 2. Each parameter acts as a “multiplier” for the production at the corresponding bus, so a value of  $u_5 = 1.2$  would set the renewable generation at bus 5 to output 20% more power than its nominal amount in the “base case”, whereas a value of  $u_{20} = 0$  would shut off the renewable generation at bus 20 altogether.

### A. System Model

The IEEE 118-bus model is a classic test case, containing 118 buses, 186 lines, and 54 generators. Descriptions of the system are widely available, e.g. from [6]. The system contains a large number of generators, but only 17 of which are actively generating more than 10 MW power. To simplify the analysis, the remaining 37 generators are taken out of service, but their respective buses are left intact. Each time power flow is solved throughout the system, reactive power limits at each generator are enforced to prevent the obvious instability caused by sinking too much reactive power into a generator.

1) *Generators*: The base power for each machine is computed by taking the  $P_{\max}$ ,  $Q_{\max}$  and  $Q_{\min}$  figures quoted in the power flow case file, and assuming that the capability of each machine is to produce up to 1.0 per-unit real power, 0.8 per-unit reactive power in over-excitation, and 0.6 per-unit in under-excitation. These are typical figures for large, transmission-level synchronous machines [7].

The dynamical model for each generator is constructed from a standard round-rotor generator model (GENROU), a standard DC exciter model (DC1A [8, Sec. 5.1]), alongside a suitably designed voltage compensator [8, Sec. 4]. Governors are generally considered to be too insensitive to initiate small-signal events, so are not modeled for this study. Identical per-unit parameters are rescaled to different machine base powers.

2) *Loads*: Loads are modeled as a mixture of 70% constant-impedance and 30% constant-current, with negligible dynamics. The constant-impedance portion models lights, heaters and appliances, as well as the various transformers and lines in the conduction path, while the constant-current portion models induction motors, which are widespread for industrial loads.

Table I: Decay rate sample statistics (units of  $10^{-2}/s$ )

Sample size	Mean	Median	Mode	Std. Dev.	Min	Max
60	3.05	3.13	3.87	0.433	1.81	3.86
600	2.99	3.02	4.28	0.421	1.43	4.28
6000	2.98	3.00	4.32	0.439	0.900	4.32
60,000	2.99	3.00	4.63	0.437	0.746	4.63
360,000	2.99	3.00	4.64	0.437	0.584	4.64

Table II: Decay rate prediction intervals (units of  $10^{-2}/s$ )

Sample size	Prediction Confidence			
	99%	99.9%	99.99%	99.999%
60	[1.89, 4.21]	[1.54, 4.56]	[1.23, 4.87]	[0.94, 5.16]
600	[1.90, 4.08]	[1.60, 4.38]	[1.34, 4.64]	[1.11, 4.87]
6000	[1.85, 4.11]	[1.54, 4.42]	[1.27, 4.69]	[1.04, 4.92]
60,000	[1.86, 4.12]	[1.55, 4.43]	[1.29, 4.69]	[1.06, 4.92]
360,000	[1.86, 4.12]	[1.55, 4.43]	[1.29, 4.69]	[1.06, 4.92]

3) *Distributed Renewables*: The vast majority of renewable resources interface with the power system through power electronics, which have near-instantaneous dynamics that can be neglected for the purposes of a transmission-level simulation. In the presence of power-point tracking mechanisms, these renewables will act as constant real power injections; without power tracking, they will behave like direct-axis current sources. In this paper, the renewable generation at each bus is modeled as 90% real power injections and 10% direct-axis current injections. Since there is no mandate in the U.S. for small, distribution-level renewables to provide reactive support, we simply assume that their reactive power contributions are negligible.

#### IV. STATISTICAL ANALYSIS

Our study begins by collecting samples of the decay rate, by drawing the uncertainty parameters  $u$  from a uniform distribution. Results are shown in Tab. I, and by assuming an underlying normal distribution, prediction intervals are computed for each sample size in Tab. II. The histogram / cumulative distribution function for the largest sample size is shown in Fig. 1.

Results show that an “average” uncertain scenario is relatively unassuming, admitting a decay rate of  $\sim 3\%$  per second, corresponding to a damping ratio of around 1-2%. On average, a high penetration of distributed renewables does not appear to significantly impact system stability, at least within the modeling assumptions contained in this paper. This result concurs with studies performed on real power systems [1], [9].

However, examining the statistics closer reveals considerable skew and kurtosis (i.e. “long-tailed-ness”) in the distribution. Table I shows that the mode differs considerably from the mean and median for all sample sizes. All five intervals predict around a 1 in 100,000 chance for a scenario to admit a decay rate being below 1% per second, but such scenarios are found in practice within just 6000 samples. While the distribution may appear to be normal at first glance, the results show that outlier cases are far more common, and this can lead to large errors when making predictions.

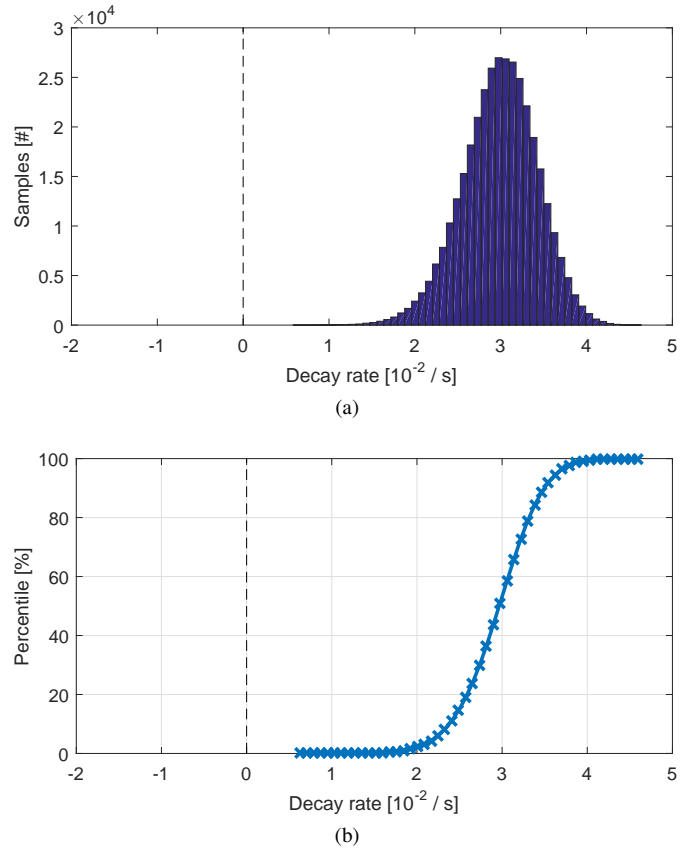


Figure 1: Distribution of decay rate over 360,000 samples: (a) histogram; (b) cumulative probability distribution.

#### V. UNSTABLE SCENARIOS VIA LOCAL OPTIMIZATION

We proceed to use local optimization techniques to probe at the worst-case scenario. Since the problem is highly non-convex, numerous local minima will be found, so the procedure should be repeated with different, randomized initial points. After 100 runs of local optimization performed using `fmincon` in MATLAB, 100 locally least-stable solutions are found. These solutions are visualized in Fig. 2, as the 0%, 25%, 50%, 75% and 100% quantiles for the  $u$  values allocated to each system bus. The solutions span a wide combined range, but many of them are closely gathered towards a median “bad-case scenario”. As shown in Fig. 3, all 100 scenarios are considerably less stable than those sampled in the previous section, deviating a remarkable 6-7 standard deviations from the mean.

It is important to validate that the instabilities found correspond to real, physical phenomena, and are not simply a manifestation of the optimizer exploiting modeling errors. We provide an illustration for the most unstable of the 100 solutions, which has an eigenvalue pair at  $\lambda = 0.002 \pm 3.9512j$ . The instability would manifest as a 0.6 Hz oscillation that grows in magnitude at a rate of 0.2% per second, or about 12% per minute. Computing the participation factors [10] reveals that only machine rotor speeds and rotor angles participate in

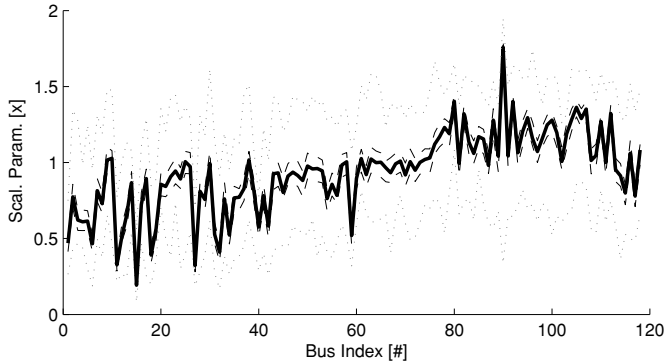


Figure 2: Solution distribution for 100 runs of local optimization. Black, solid: median; black, dashed: 25% and 75% quantiles; gray, dotted: 0% and 100% quantiles.

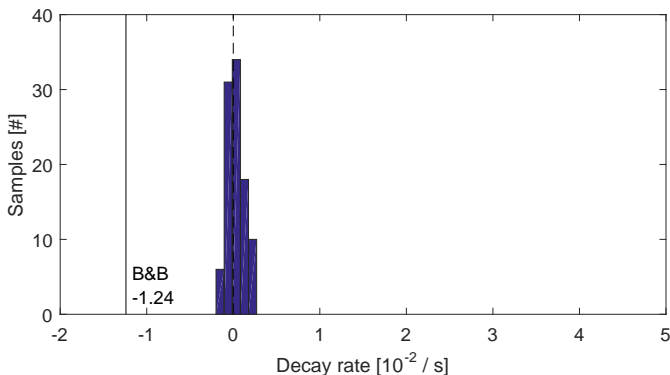


Figure 3: Histogram of damping rates for 100 locally least-stable scenarios found via local optimization. The least stable scenario has a damping rate of  $-0.002s^{-1}$ , and branch-and-bound on the order-reduced, linearized approximation predicts  $\alpha \geq -0.0124s^{-1}$  in the neighborhood of these scenarios.

the unstable modes. The most affected machines at bus 25 and bus 111, which are located at opposite extremes of the network. These are all tell-tale signs of interarea oscillation; indeed the suspicion is confirmed using time-domain simulation, as shown in Fig. 4.

## VI. STABILITY GUARANTEES

In the previous section, local optimization was successful in catching several unstable or nearly-unstable outlier scenarios. But both local optimization and statistical analysis will inevitably fall short in making conclusive predictions about the true worst-case scenario. Both methods leave us wondering whether there is a significantly less stable scenario that is simply overlooked.

To this end, an important idea from robust control theory is the *stability certificate*, which provides a lower-bound on the decay rate for all uncertain scenarios of a given model, i.e.

$$\underline{\alpha} \leq \min \mathcal{D}, \quad (6)$$

where  $\mathcal{D}$  was previously defined in Section II. Essentially, the stability certificate guarantees a minimum amount of

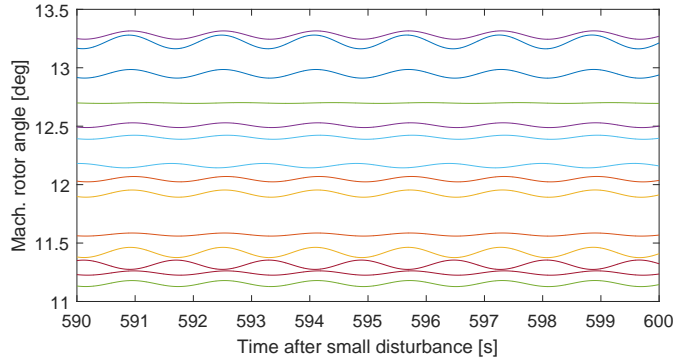


Figure 4: Time domain simulation of the rotor angles after a small disturbance. The oscillations are undamped and grow slowly in magnitude.

damping for *every eigenmode of every uncertain scenario*. A certificate for  $\underline{\alpha} > 0$  immediately guarantees that every uncertain scenario—even the worst-case—will remain stable.

Stability certificates are difficult to compute, often requiring computational effort that grows exponentially with the size and complexity of the given model. Also, the predictions made can be conservative, and this conservatism can adversely impact their usefulness (e.g. a certificate for  $\underline{\alpha} = -\infty$  would be relatively meaningless). The easiest models to work with are those whose Jacobian matrices  $A_u, B_u, C_u, D_u$  have a linear dependence on the uncertain parameters—a structure sometimes known as linear parameter varying (LPV). In these cases, relatively nonconservative stability certificates can be computed for models containing up to 100 states and 10 dimensions of uncertainty, and more dimensions of uncertainty can be accommodated at the expense of increasing conservatism [11], [12].

The problem is significantly more difficult for models with a nonlinear dependence on uncertain parameters. Using sum-of-squares methods, stability certificates can be constructed for these models containing up to 10-20 combined dimensions of states and dimensions [13].

### A. Low-dimensional LPV Approximation

The model developed in this paper has a nonlinear dependence on the uncertain parameters, due to the need to resolve power flow for each new choice of renewables production. It also contains 97 state variables and 118 uncertain parameters, which puts sum-of-squares methods entirely out of reach. Instead, we proceed to *approximate* the nonlinear parameter dependence by linearizing about an operating point, thereby yielding an LPV model. The physical intuition is to replace the a.c. power flow equations with the “d.c. power flow” analogs. Such an approximation is widespread in power systems, and are used to formulate optimal power flow [14] and unit commitment [15] problems as linear and mixed integer programs.

Since all of the unstable scenarios found via local optimization have similar values of  $u$ , it makes sense for our LPV model to be most accurate over the values of  $u$  covered by

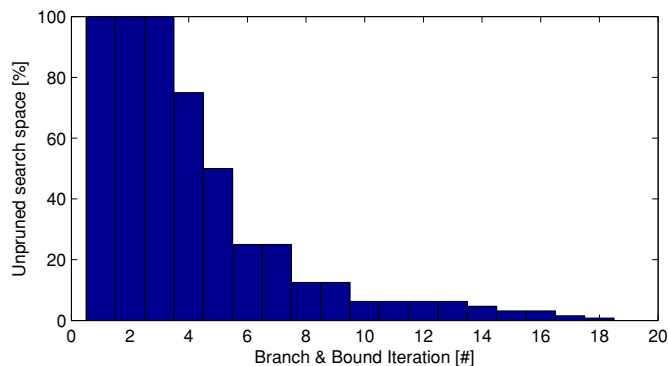


Figure 5: Progress of branch & bound as applied to the linearized model. Each iteration took between 2,000-4,000 s on a 16-core Intel Xeon E5 CPU.

the unstable points found via local optimization. Following this, the LPV approximation is constructed by expanding about the median of the 100 outlier scenarios found via local optimization, and estimating each gradient using centered finite differences. The resulting LPV approximation has 118 uncertain parameters, most of which are redundant in describing the underlying uncertainty. Applying order reduction techniques, we find that just 7 dimensions of uncertainty (i.e. principal components) are needed to capture the behavior of the LPV model to an approximation error of below 1%.

### B. Computation of Lyapunov Certificates

Vertex-based Lyapunov stability certificates [12, Eqn. 5.8] are computed for the LPV model with 7 dimensions of uncertainty, and a branch-and-bound scheme is used to refine the conservatism of the bound [16]. The final result is shown alongside the decay rates of the unstable scenarios found via local optimization in Fig. 3. The certificate predicted a decay rate lower-bound of  $-0.0124/s$ , suggesting that the worst-case scenario should not be too much worse than the outlier scenarios already found using local optimization.

Despite the use of a reduced LPV approximation, the stability certificate still required a significant amount of computational effort. Branch-and-bound converged in 19 iterations (shown in Fig. 5), but each iteration required the solution of a conic optimization problem with  $97^2 = 9409$  primal decision variables and  $2^7 \cdot 97^2 \approx 1.2 \times 10^6$  dual decision variables. This took around an hour each time, even when using application-specific, custom-tailored codes on expensive hardware, and the combined running time for all 19 iterations was around a full day.

## VII. CONCLUSION

This paper provides a case study to highlight the importance of stability verification/certification techniques in analyzing the impact of distributed renewables on the small-signal stability of the transmission system. Statistical methods can underestimate the impact of outlier scenarios, some of which can be found using local optimization, but only a stability certificate

can exhaustively guarantee that all outlier scenarios will remain stable. In practice, the computational power required to compute the stability certificates is formidable, even for the linearized, order-reduced approximation to a small 118-bus system. Further progress in theoretical and computational methods are needed to scale theory to realistic-sized problems, which may contain tens of thousands of buses and thousands of generators. This is an important area of future research.

## VIII. ACKNOWLEDGMENTS

The authors thank F. Ma and E. Litvinov for enlightening discussions. Partial financial support for this work was provided by the MIT Energy Initiative and the Skolkovo-MIT Initiative in Computational Mathematics.

## REFERENCES

- [1] B. Tamimi, C. Canizares, and K. Bhattacharya, "System stability impact of large-scale and distributed solar photovoltaic generation: The case of ontario, canada," *Sustainable Energy, IEEE Transactions on*, vol. 4, no. 3, pp. 680–688, 2013.
- [2] R. Shah, N. Mithulananthan, R. Bansal, and V. Ramachandramurthy, "A review of key power system stability challenges for large-scale pv integration," *Renewable and Sustainable Energy Reviews*, vol. 41, pp. 1423–1436, 2015.
- [3] J. L. Rueda, D. G. Colomé, and I. Erlich, "Assessment and enhancement of small signal stability considering uncertainties," *Power Systems, IEEE Transactions on*, vol. 24, no. 1, pp. 198–207, 2009.
- [4] R. Preece, K. Huang, and J. Milanovic, "Probabilistic small-disturbance stability assessment of uncertain power systems using efficient estimation methods," *Power Systems, IEEE Transactions on*, vol. 29, no. 5, pp. 2509–2517, Sept 2014.
- [5] P. Apkarian and D. Noll, "Nonsmooth  $H_\infty$  synthesis," *Automatic Control, IEEE Transactions on*, vol. 51, no. 1, pp. 71–86, Jan 2006.
- [6] R. Christie. (2000) Power systems test case archive. [Online]. Available: <https://www.ee.washington.edu/research/pstca/>
- [7] J. Jackson, "Interpretation and use of generator reactive capability diagrams," *Industry and General Applications, IEEE Transactions on*, no. 6, pp. 729–732, 1971.
- [8] D. Lee, "Ieee recommended practice for excitation system models for power system stability studies (ieee std 421.5-1992)," *Energy Development and Power Generating Committee of the Power Engineering Society*, 1992.
- [9] S. Eftekharijrad, V. Vittal, G. T. Heydt, B. Keel, and J. Loehr, "Small signal stability assessment of power systems with increased penetration of photovoltaic generation: A case study," *Sustainable Energy, IEEE Transactions on*, vol. 4, no. 4, pp. 960–967, 2013.
- [10] G. Verghese, F. Schweppe *et al.*, "Selective modal analysis with applications to electric power systems, part i: Heuristic introduction," *Power Apparatus and Systems, IEEE Transactions on*, no. 9, pp. 3117–3125, 1982.
- [11] J. Doyle, "Analysis of feedback systems with structured uncertainties," in *IEE Proceedings D (Control Theory and Applications)*, vol. 129, no. 6. IET, 1982, pp. 242–250.
- [12] S. P. Boyd, L. El Ghaoui, E. Feron, and V. Balakrishnan, *Linear matrix inequalities in system and control theory*. SIAM, 1994, vol. 15.
- [13] D. Henrion and J.-B. Lasserre, "Convergent relaxations of polynomial matrix inequalities and static output feedback," *Automatic Control, IEEE Transactions on*, vol. 51, no. 2, pp. 192–202, 2006.
- [14] A. Monticelli, M. Pereira, and S. Granville, "Security-constrained optimal power flow with post-contingency corrective rescheduling," *Power Systems, IEEE Transactions on*, vol. 2, no. 1, pp. 175–180, 1987.
- [15] H. Ma and S. Shahidepour, "Unit commitment with transmission security and voltage constraints," *Power Systems, IEEE Transactions on*, vol. 14, no. 2, pp. 757–764, 1999.
- [16] V. Balakrishnan, S. Boyd, and S. Balemi, "Branch and bound algorithm for computing the minimum stability degree of parameter-dependent linear systems," *International Journal of Robust and Nonlinear Control*, vol. 1, no. 4, pp. 295–317, 1991.